Synthesis of Magnetic Nanoparticles Coated with Human Serum Albumin and Loaded by Doxorubicin

Kirill Petrov, Elena Ryabova, Elena Dmitrienko and Alexey Chubarov

Institute of Chemical Biology and Fundamental Medicine SB RAS, 630090 Novosibirsk, Russia

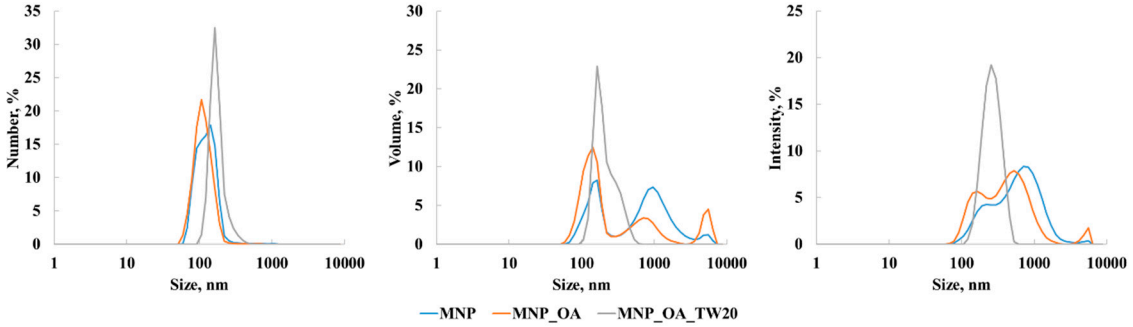


Figure S1. The hydrodynamic diameter of MNP, MNP_OA, and MNP_OA_TW20 by DLS in three distribution modes: Number, Volume, and Intensity.

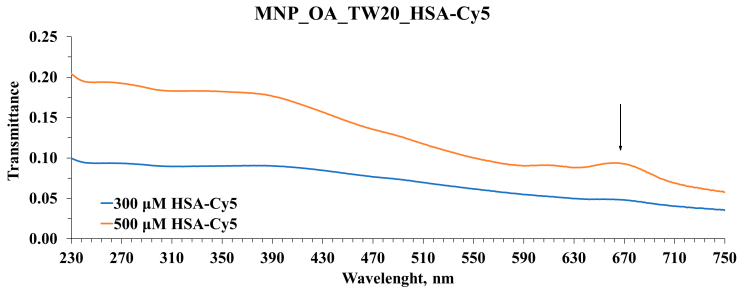


Figure S2. UV-vis spectra of MNP_OA_TW20_HSA-Cy5 in deionized water. The Cy5 peak is marked with an arrow. The NPs were obtained with 0.3- and 0.5-mM HSA-Cy5 during the protein loading procedure at pH 7.4.

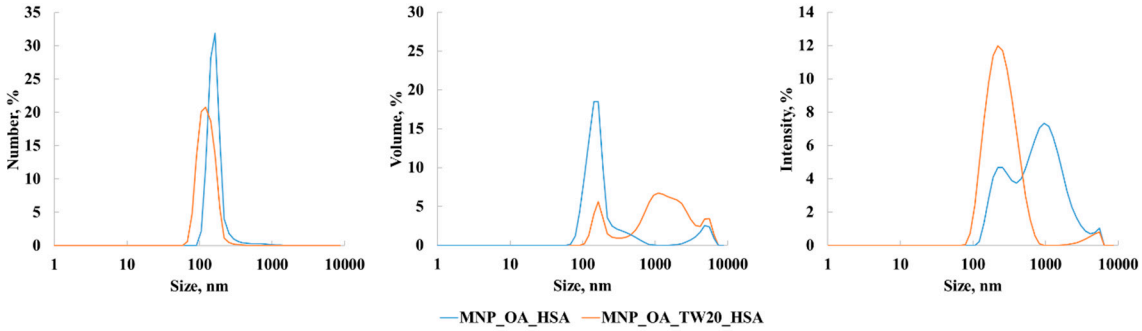
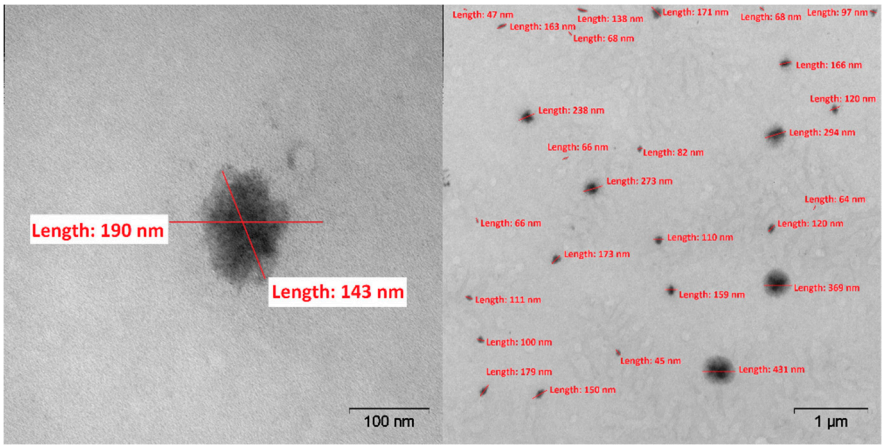


Figure S3. The hydrodynamic diameter of MNP_OA_HSA and MNP_OA_TW20_HSA by DLS in three distribution modes: Number, Volume, and Intensity.



(a) **(b)**

Figure S4. Representative TEM images of MNP_OA_HSA and MNP_OA_TW20_HSA, high (a) and low (b) magnification.

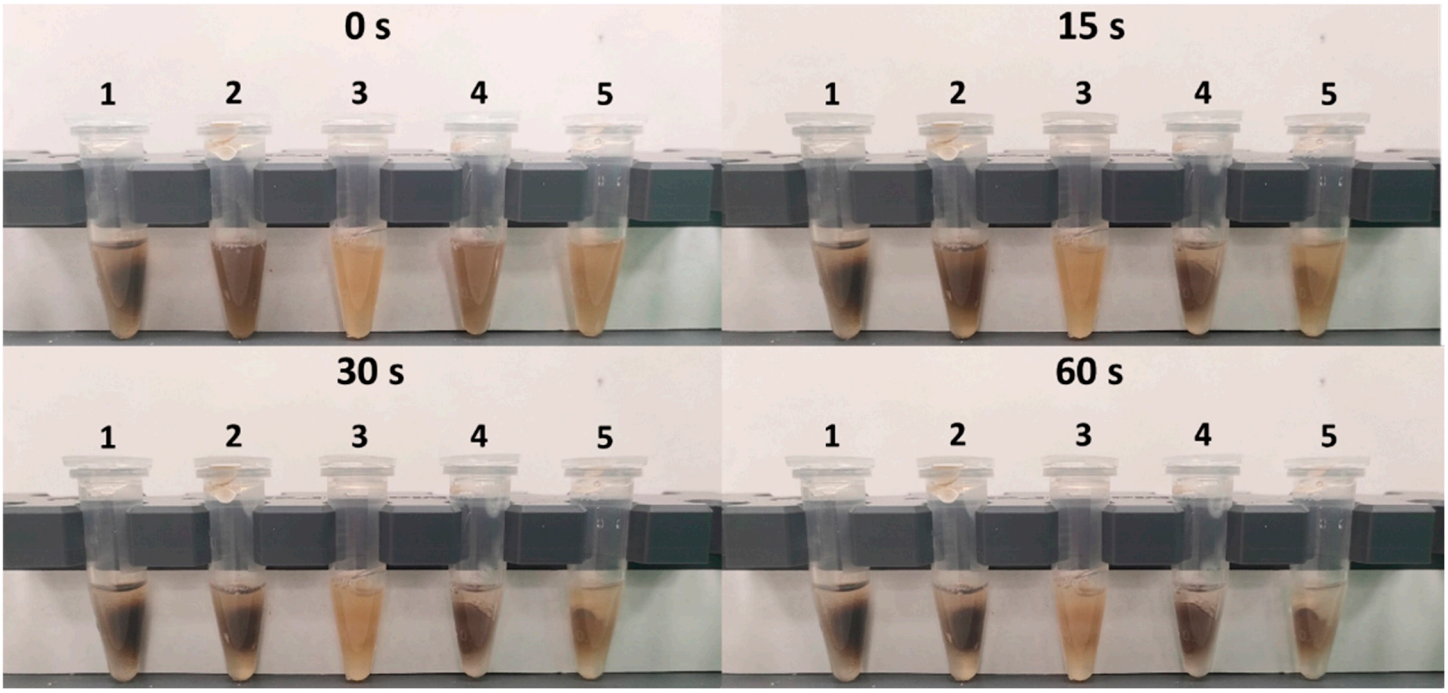


Figure S5. MNPs in mQ water on the magnetic rack at various time points. 1 ─ MNP, 2 ─ MNP_OA, 3 ─ MNP_OA_TW20, 4 ─ MNP_OA_HSA, 5 ─ MNP_OA_TW20_HSA

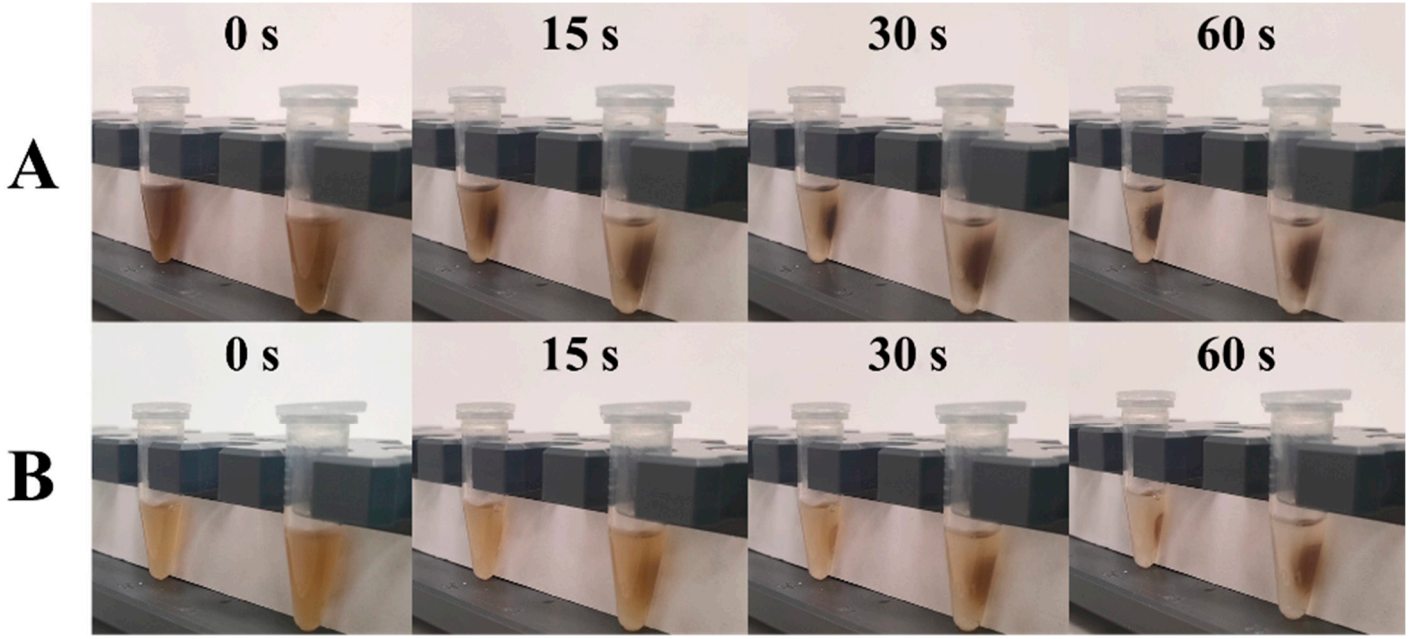


Figure S6. MNP_OA (A) and MNP_OA_TW20 (B) without (left) and with HSA-coating (right) in mQ water on the magnetic rack at various time points.

The relaxivities r_1 and r_2 were found by finding the tangent of the slope of the inverse of T_1 or T_2 proton relaxation times per iron concentration (Figure S5).

$$\frac{1}{T_i} = \frac{1}{T_{i,d}} + r_i \cdot C_{Fe},$$

where T_i is the measured relaxation time, $T_{i,d}$ is the diamagnetic solvent contribution.

For MNP_OA and MNP_OA_TW20, a simplification for Fe concentration calculation was used that nanoparticles consist only of magnetite. For HSA-coated nanoparticles, Fe concentration was evaluated in the albumin capacity. The graphs presented below show the dependence of 1/T on the concentration of iron. Data presented on these graphs was approximated by linear function: $y = a \cdot x + b$. The slope of the linear function equals the relaxivity.

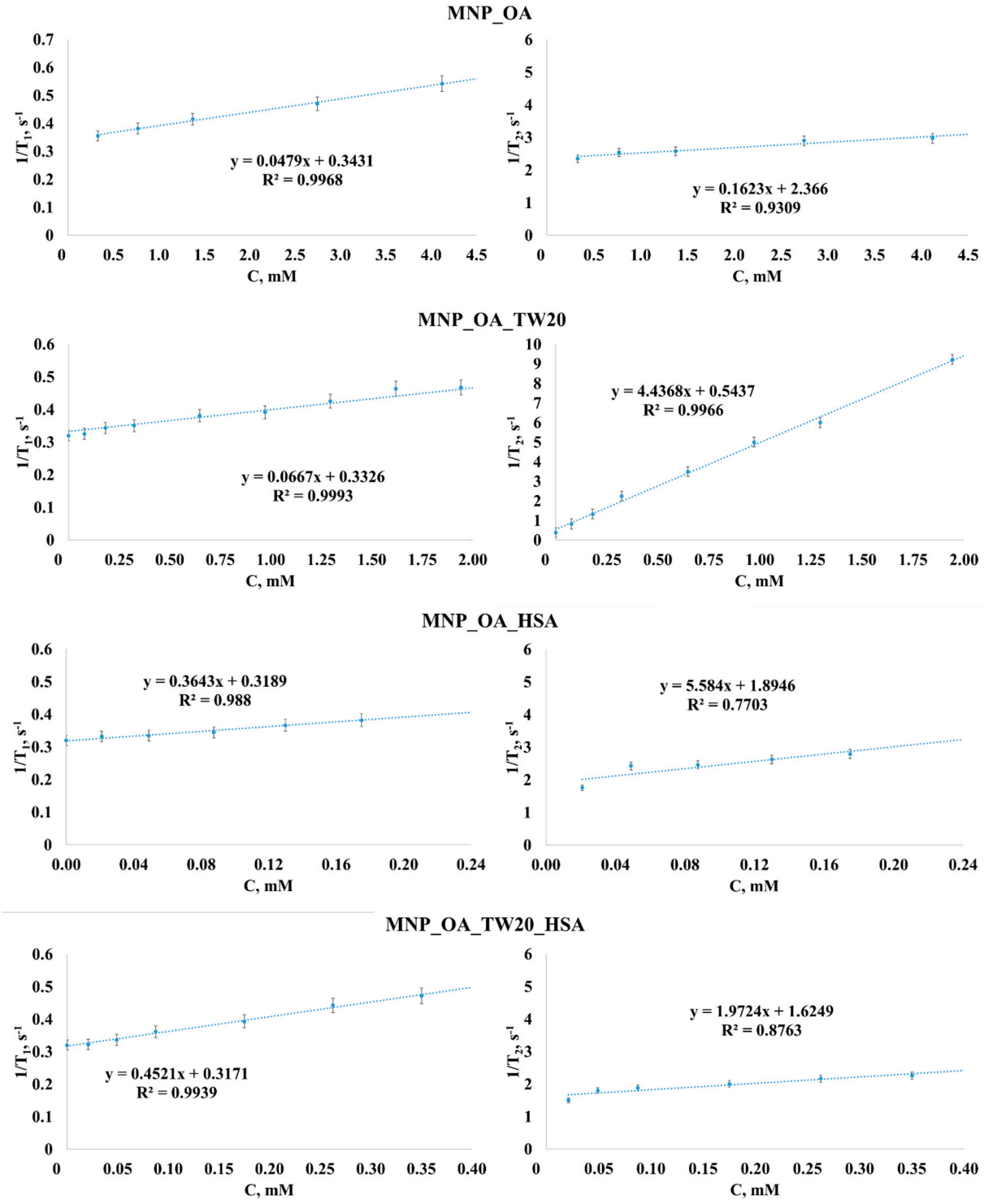


Figure S7. Relaxivity (r_1 and r_2) calculations under a magnetic field of 1.88 T.

To study kinetics, DOX release was evaluated with different general kinetics models, such as first-order, Higuchi, and Korsmeyer–Peppas (Table S1). Common metrics for agreement of fit with each kinetics model were then calculated (R^2). The equations for the kinetics model are as follows:

1) first-order $C_{DOX} = C_{DOX\infty} \times (1 - e^{-k1t})$
2) Higuchi $C_{DOX} = k_H \times t^{1/2}$
3) Korsmeyer–Peppas $C_{DOX}/C_{DOX\infty} = k_{KP} \times t^n$

where C_{DOX} is the amount of DOX released at time t, $C_{DOX\infty}$ is the amount of drug release at infinite time, n is the exponent, and k_1, k_H, and k_{KP} are the first-order, Higuchi, and Korsmeyer-Peppas release constants, respectively.

Table S1. Correlation coefficients and release parameters based on drug release data (Figure 13).

NP	pH	First-order		Higuchi		Korsmeyer-Peppas		
		k_1, min^{-1}	R^2	k_H, $M/min^{1/2}$	R^2	k_{KP}, min^{-n}	n	R^2
MNP_OA_HSA	4.5	0.017	0.862	$2.4 \cdot 10^{-6}$	0.960	0.45	0.10	0.999
	5.5	0.011	0.836	$1.8 \cdot 10^{-6}$	0.950	0.34	0.10	0.999
	7.4	0.008	0.841	$1.5 \cdot 10^{-6}$	0.950	0.29	0.09	0.999
MNP_OA	4.5	0.013	0.875	$1.8 \cdot 10^{-6}$	0.963	0.34	0.12	0.999
	5.5	0.009	0.899	$1.4 \cdot 10^{-6}$	0.975	0.21	0.18	0.999
	7.4	0.007	0.834	$1.2 \cdot 10^{-6}$	0.949	0.25	0.10	0.999
MNP_OA_TW20_HSA	4.5	0.024	0.885	$2.3 \cdot 10^{-6}$	0.959	0.48	0.12	0.999
	5.5	0.012	0.863	$1.6 \cdot 10^{-6}$	0.960	0.33	0.13	0.999
	7.4	0.010	0.894	$1.3 \cdot 10^{-6}$	0.970	0.27	0.13	0.999
MNP_OA_TW20	4.5	0.009	0.875	$7.7 \cdot 10^{-7}$	0.970	0.26	0.13	0.999
	5.5	0.012	0.862	$9.6 \cdot 10^{-7}$	0.960	0.33	0.12	0.999
	7.4	0.008	0.885	$7.5 \cdot 10^{-7}$	0.972	0.25	0.12	0.999